Islamic Azad University
Mashhad Branch

Arjmandzadeh et al / Iranian Journal of Earth Sciences 9 (2017) / 39-47

Satellite thermal surveys to detecting hidden active faults and fault termination, Case study of Quchan fault, NE Iran

Reza Arjmandzadeh[*1], Vahid Shafiei Rashvanlou[1], Rahim Dabiri[2], Alireza Almasi[3]

1. Department of Geology, Payame Noor University (PNU), Iran
2. Department of Geology, Mashhad Branch, Islamic Azad University, Mashhad, Iran
3. Department of geology, Lorestan University, Khorramabad, Iran

Received 10 May 2016; accepted 4 January 2016

Abstract

The Quchan fault is located in Quchan - Shirvan area which is a part of Chenaran- Bojnourd plain in Kopeh-Dagh zone, NE Iran. The Quchan active fault with northwest – southeast trending is one of the most important strike-slip faults in the area which its activity led to the numerous historical and instrumental earthquakes. The Neo-tectonic activities of this fault are investigated by the drainage patterns, displacement of the waterways, the impact on the alluvial fan deposits and the Quaternary sediments cutting. Here, we aim to employ instrumental seismicity along with satellite imagery data, thermal images, shuttle radar topography mission (SRTM) data plus field observations to explain the mechanism and active tectonics of the southeast Quchan fault termination. Processing Landsat-8 image synchronous with the maximum micro-seismic occurrences reveals that thermal anomaly is positive and corresponds to the major lineaments. Thermal anomaly images have also revealed three hidden faults which have not yet been distinguished in the field surveys. The continuous strike slip activity of the Quchan fault over the time resulted in the formation of compression zone and new thrusts along the southeastern end. By continuance of thrust activity, the anticline starts to accrete and the older thrusts are covered with folding sedimentary rocks, thus thrust loader continues until now. This research is the first successful attempt in Iran to detect hidden active faults and investigate fault termination by employing satellite thermal surveys.

Keywords: *Quchan fault, Kopeh-Dagh, drainage pattern, micro seismic, Landsat-8, thermal anomaly.*

1. Introduction

The system of NNW–SSE right-lateral strike-slip faults in the Bakhardan–Quchan fault zone between Bojnurd and Quchan is one of the most prominent structural and topographic features of the central Kopeh Dagh zone (Fig. 1). Most of the fault segments were mapped on regional scale geological maps (Huber 1977; Afshar Harb 1979; Afshar Harb et al. 1987; Robert et al. 2014) in which the Quchan fault is considered as one of the most dominant structure. The Quchan fault is extended to the Quchan-Shirvan area in the south east. The faults within this zone are expressed clearly in the geomorphological studies (Tchalenko 1975; Hollingsworth et al. 2006; Hollingsworth et al. 2008; Shabanian et al. 2009).

In the history of seismo-tectonic thermal infrared research, it is undeniable that before and after strong earthquakes and micro-seismic occurrences, there are significant thermal infrared anomalies which have been interpreted as preseismic precursor in earthquake prediction and forecasting (Bhardwaj et al., 2017). The methodology has been first aimed at understanding the mechanism of Quchan fault termination and the relationship between the satellite thermal anomaly and earthquake density and the active faulting and folding in these earthquakes. In this paper, we use instrumental seismicity along with observations from satellite imagery data, thermal images, SRTM topographic data plus field observations of the landforms to explain the mechanism and active tectonics of the southeast Quchan fault termination. These different data types cover a range of timescales of deformation, enabling us to identify the most important features, and to reveal patterns, which would otherwise be difficult to see. The aim is to better understand the deformation occurring along strike-slip fault termination and detect hidden active fault. An important by-product of this work is a better understanding of the relationship between seismic hazard and thermal anomaly when the earthquake density is high in this region (Kim et al., 2004; Cunningham & Mann, 2007).

We first describe the geomorphology of the faulting and the mechanism of Quchan fault termination using remote sensing data and finally detect the hidden faults with thermal anomaly produced by high density of micro seismic activity on the fault termination.

---

*Corresponding author.
E-mail address (es): arjmand176@gmail.com

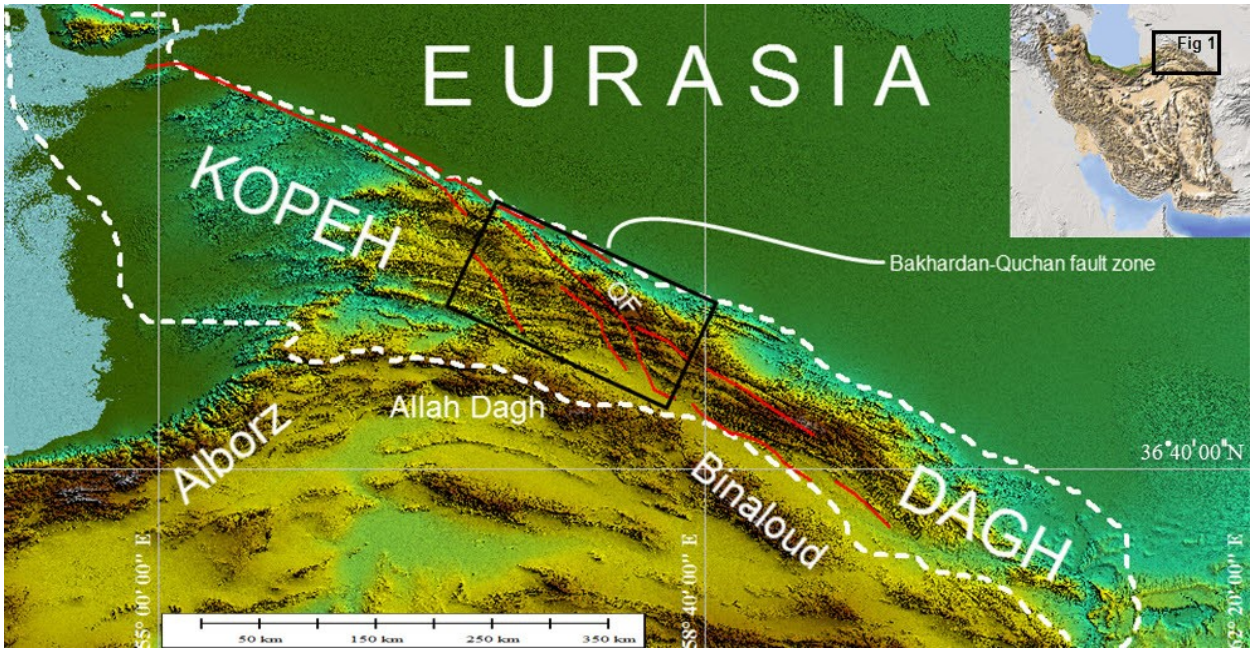

Fig. 1. SRTM digital topographic image of the Kopeh Dagh Zone in the Arabia-Eurasia collision framework that showing the Bakhardan-Quchan location in the tectonic context of NE Iran. The Quchan fault trending is shown in image. Abbreviation is QF, Quchan fault.

2. Remote sensing methodology

Satellite images are widely used to identify different geological landforms and structures such as faults and lineaments (Vrabel 1996). The enhanced thermal infrared (TIR) emission from earth's surface retrieved by satellites prior to earthquakes is known as "thermal anomaly" (Freund et al. 2005). The idea that thermal anomalies may be associated with seismic activity was put into application in Russia, China and Japan. In 1980, Russian scientists detected thermal anomalies before an earthquake occurs in Central Asia employing satellite images (Tronin 1996). Then, other researchers reported more evidence on thermal anomalies before strong earthquakes (Choudhury et al., 2006). In several studies, obvious correlations of thermal anomalies in land surface temprature (LST) related to pre-seismic activities have been observed (Saraf and Choudhury 2005; Choudhury et al. 2006; Pulinets et al., 2006). The methodologies for this research are divided into the following steps:

- The micro-seismic data (about 600) from International Institute of Earthquake Engineering and Seismology (IIEES) were plotted on Satellite images.
- The OLI and TIR sensor images are used to detect lineaments. In order to enhance the spatial resolution of satellite image, band 8 of OLI sensor with spatial resolution of 15 meters combined with other bands with 30 meter spatial resolution using the pan sharpening method till the effects were detected with higher accuracy.
- The visual analysis and filtering methods have been used to identify and distinguish the faults and landforms. In visual analysis, shifting rock units, identification of the valleys and ridges in a straight line, the sharp displacement of rivers and streams, vegetation cover in a particular direction and faults and lineaments can be identified to a certain extent due to changes in the tone of satellite images, but some of these complications should be identified with image processing methods such as filtering (Sabins 1998).
- Directional filters used in this study to detect lineaments which generally have widespread and prevalent usage in geology. In this method, satellite imagery is filtered with Sun directional method in 4 directions (N-S, NE-SW, E-W and NW-SE) to detect the linear traces and remove data with high error probability.
- Consequently, to discriminate major and minor faults, the parameters such as the faults length, the displacement along faults trend along with the literature data are used. Finally, we determined faults mechanism considering their criteria in satellite imagery and field evidence.

3. Geological and structural framework

Many researchers estimated the convergence rate between the Iranian and Turan plates 22-50 mm/year (McKenzie 1972; Allen et al. 2004; Vernant et al. 2004). The shortening rate of Kopeh-Dagh along the north-south has also been reported about 16 mm/year (Lyberis and Manby 1999). Tchalenko (1975) illustrated

the Kopeh-Dagh tectonic and its fault formations based on the movement of Iranian plate towards Turan plate leading to the NNE compression.

One of the major faults in Kopeh-Dagh zone that have impact on these displacement is the Quchan fault (Hollingsworth et al. 2006). The Quchan fault is the longest segment and the major strike-slip fault in the Bakhardan-Quchan fault zone in Kopeh-Dagh. This fault extends from the city of Quchan in the southeast to 24 km north of Garmab village in the northwest and turns obliquely into the main Kopeh-dagh fault zone (MKDF). Moreover, it creates thrust fault system in the southeast termination in north of Quchan city (Fig. 2).

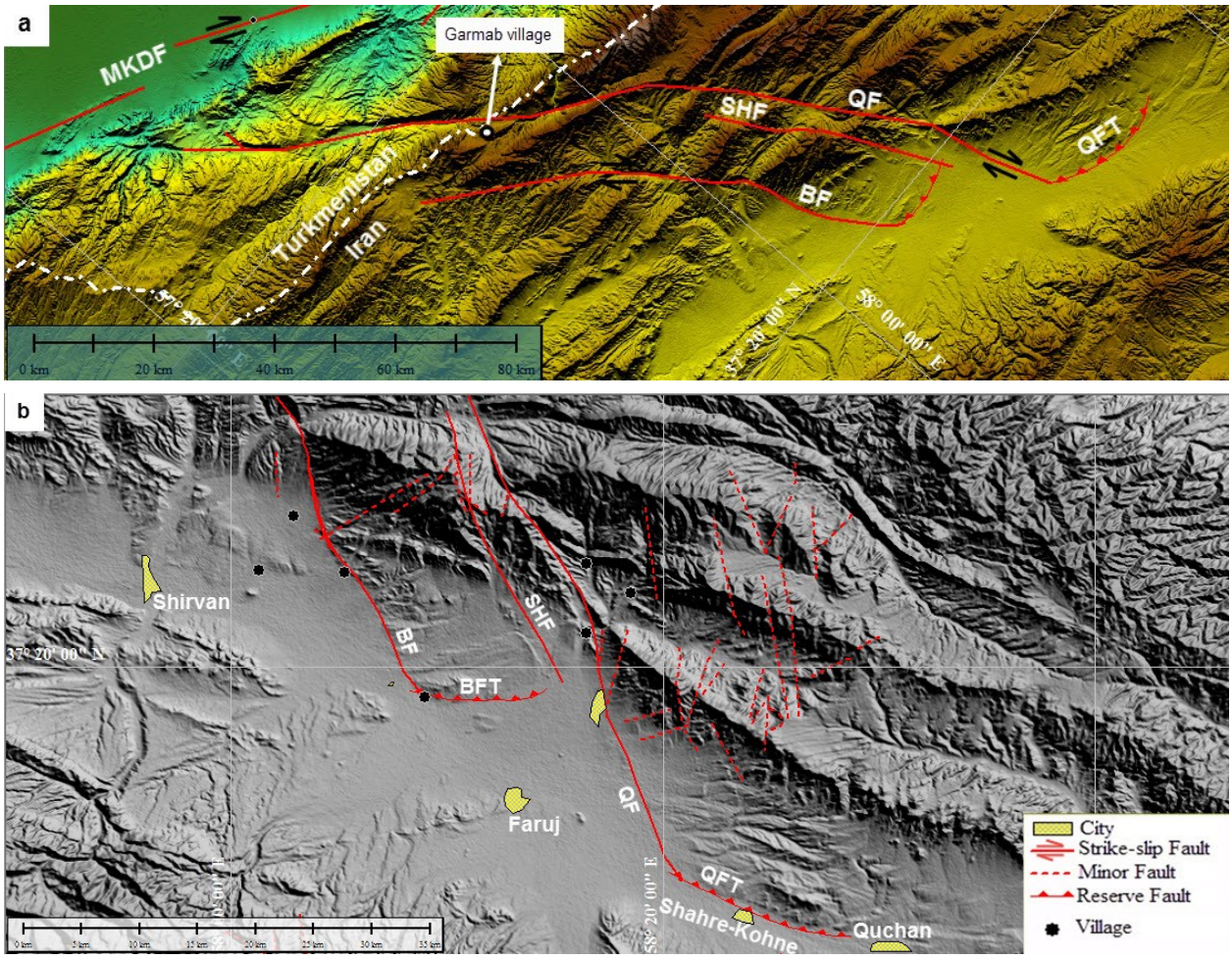

Fig. 2. (a) SRTM digital topographic image of NE Iran with the main faults of the Bakhardan-Quchan fault zone. The Quchan fault trending is shown on image. The Quchan fault extends from southeast to 24 km north of Garmab village in the northwest. (b) GTOPO30 topographic image of Quchan-Shirvan area with the trending of main faults. Uplift and folding in southeast Quchan fault termination can be seen in image. Abbreviations are MKDF, Main Kopeh Dagh Fault; QF, Quchan fault; BF, Baghan fault; SHF, Shokranlou fault. QFT, Quchan fault termination; BFT, Baghan fault termination.

Remote sensing data indicate that the dominant activity of the fault is right lateral strike-slip movement (Fig. 3). As characteristic trace, displaced geomorphological markers such as alluvial fans, beheaded drainages and offset active streambeds, indicate Quaternary activity along much of its length (Fig. 3). In contrast to the southern limit, the northern termination of Quchan fault was mapped clearly in previous studies (Hollingsworth et al., 2008). Geomorphological evidence and subtle remote sensing results indicating its thrust-bend termination in the Shahre-kohne village (Fig. 3) near the city of Quchan.

This fault obliquely cuts the landforms and topographic structure of the Kopeh-Dagh zone and displaces the rock units in clear right-lateral offsets (Fig. 3). In the north, it turns obliquely into the MKDF (Fig. 2). An illustration of remote sensing is shown in Fig. 3, where the offset across the Quchan fault is measured. Excellent bedrock exposure, visible in the satellite imagery, allows a convincing reconstruction of 15 km total right-lateral motion.

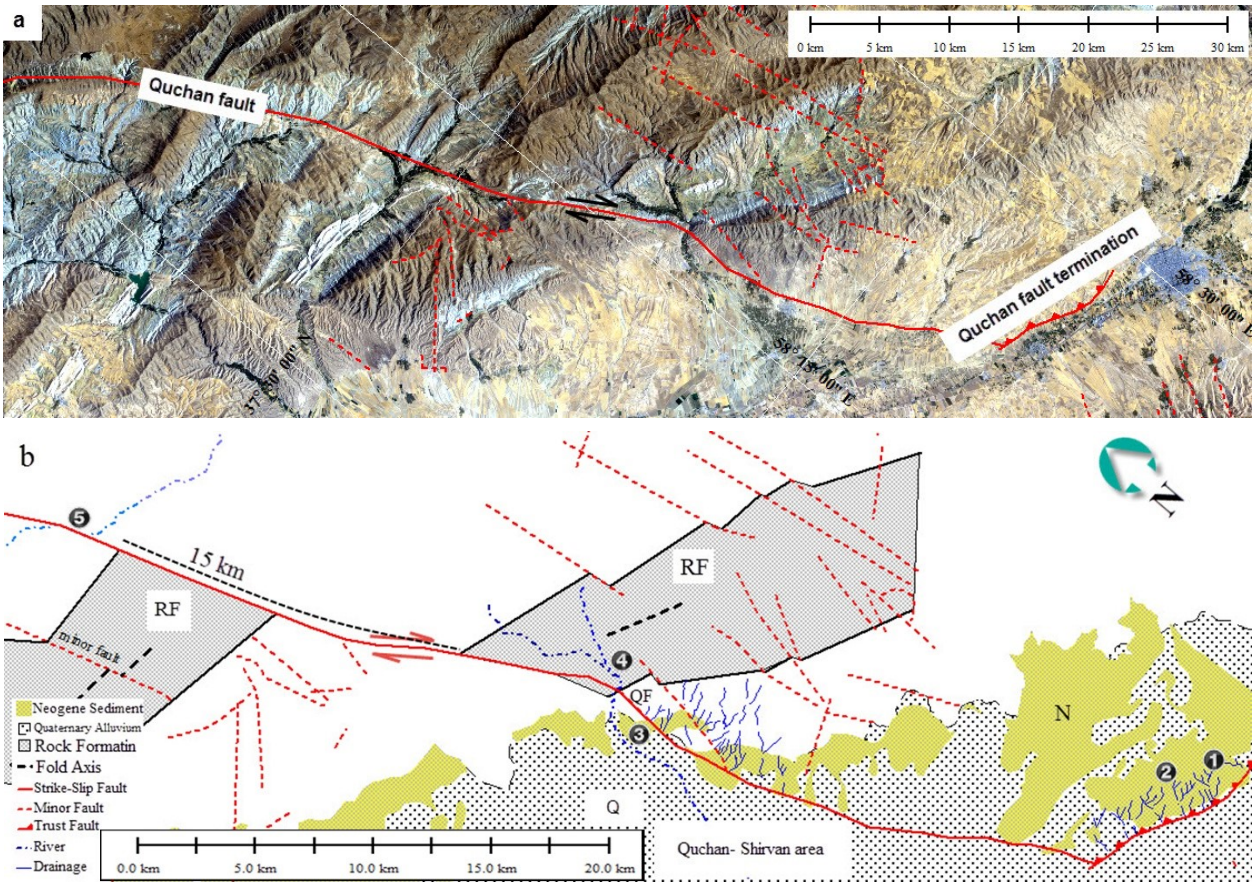

Fig. 3. (a) Landsat-8 (531) imagery of Quchan fault trend. (b) Morpho-tectonic map of the Quchan fault zone based on (a). The offset value in folded rock formation is expressed in kilometer. Numbers represent the Quchan fault Neotectonic effects. RF, Rock Formation; N, Neogene Sediment; Q, Quaternary Alluvium.

4. Quchan fault termination

Just in the north of Old Quchan (Shahre-Kohne village) is an anticline known as the Quchan anticline (Afshar Harb et al. 1987) including uplifted Neogene, Quaternary alluvium and Cretaceous limestone (Fig. 4a and d). In the field, the southern side of the Quchan anticline displays uplifted terraces of the Atrak River. These evidence can be observed emerging from the current flood plain in the west, reaching a maximum height near old Quchan, and then dying away back to the active flood plain in the east. The higher terraces are tilted more than the lower, thus forming different levels of diverging fan in cross section (Fig. 4d) indicating that their uplift must have a local cause, rather than to be a response to a regional change in base level. Along the front of the anticline, one prominent terrace level is capped by a cemented limestone conglomerate (Fig. 4e), which accentuates its morphology.

It seems likely that a blind thrust fault runs along the southern side of the Quchan anticline, causing the area to uplift to the north. This interpretation is supported by the drainage pattern itself (Discussed in thermal anomaly and drainage pattern sections; Fig. 7a). Evidence from the landforms strongly suggest that the Quchan anticline is an active structure, uplifting as a result of a north-dipping thrust fault. Its location at the southern end of the clear morphological expression of the Quchan strike-slip fault, and on its eastern side, suggests that it represents the structural termination of the strike-slip fault.

Landsat-8 imagery thermal anomaly detected many hidden faults in the Quchan fault termination that have not yet been distinguished in the field surveys. It is noticeable that a compression zone is formed in the north of Shahre-Kohne village, near the Quchan city as a result of the right-lateral strike-slip activities of Quchan fault and redirect of fault trend in southeast termination (Fig. 5).

5. Satellite thermal anomaly

One of the most important evidence testifying that the Quchan anticline is active and uplifting as a result of north-dipping Quchan thrust fault termination is the operation of hidden faults which are evident in thermal anomaly images. Most research on active tectonics and earthquake, indicate that there are undeniably thermal infrared anomalies before and after strong earthquakes which have been interpreted as pre-seismic precursor in

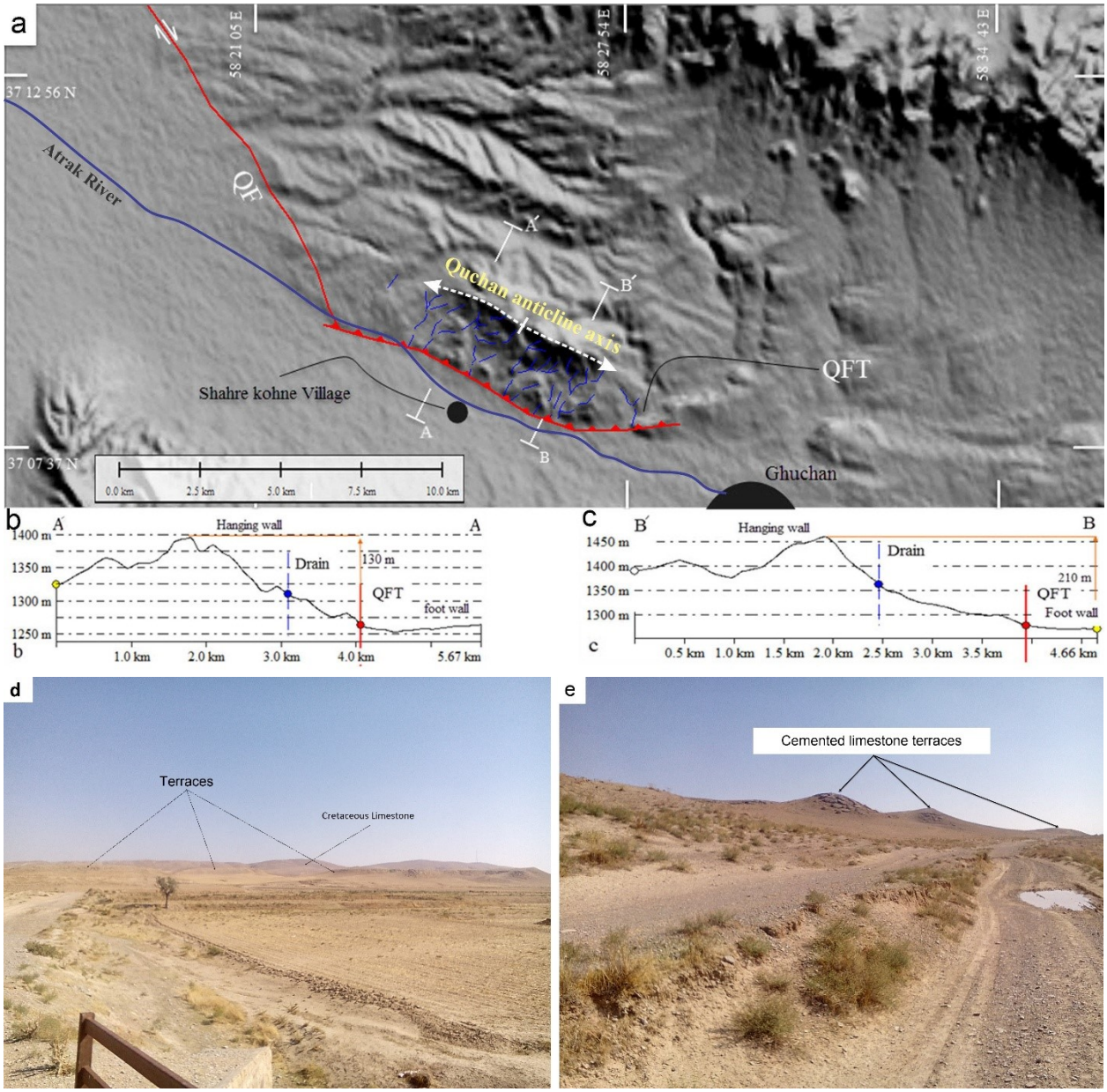

Fig. 4. (a) SRTM topography of the southeastern Quchan fault termination and the Quchan anticline with the prominent terrace along the thrust fault due to the formation of a compression zone. QF, Quchan fault; QFT; Quchan fault termination. Profiles (b) and (c) represent mean elevation along 3 km wide of anticline north western and south eastern on the profile lines in (a). Scales in elevation are in meters and in distance are in kilometers. (d) Field photograph of Quchan anticline with the terraces. (e) NE view from the front of Quchan anticline, where a prominent terrace level capped by a limestone breccia can be seen along the southern front of the Quchan anticline.

earthquake prediction and active faults (Akhoondzadeh 2014; Lu et al. 2016; Bhardwaj et al. 2017). Landsat-8 thermal images indicate the presence of positive thermal anomalies that are associated with the large linear structures and fault systems of the Earth's crust. The relation between thermal anomalies and micro-seismic activity is substantiated for the study area. Image processing includes standard procedures for Landsat-8 thermal infra-red images such as data extraction, calibration, radiation and atmospheric corrections. After these steps, temperature images of the Earth surface (LST) and thermal anomaly were obtained (Fig. 6).

The average value and standard deviation for background area were calculated for the Landsat-8 image of October 2016 synchronous with the maximum micro-seismic occurrences. All pixels in similar meteorological conditions with a temperature greater than average value of two standard deviation are considered as a thermal anomaly. Every zone in Quchan-Shirvan area has its own background and

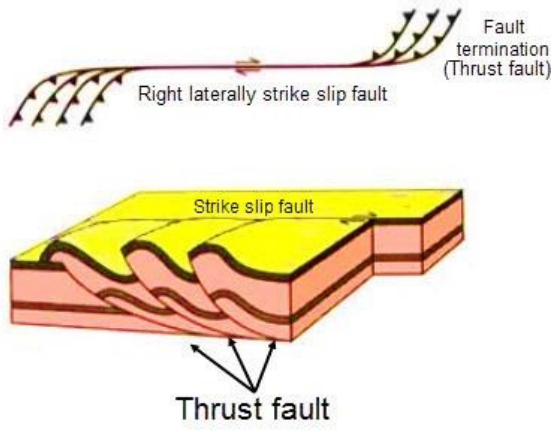

Fig. 5. Mechanism of thrust formation in the right-lateral strike-slip fault termination.

thermal anomaly. Hence we have analyzed only positive anomalies. Water surfaces and clouds were masked and excluded. As a result, the thermal anomaly image and the surface temperature of the earth were obtained (Fig. 6).

According to the obtained results, the temperature in the area is high on average because of maximum occurrences of micro-seismic earthquakes in October 2016. The thermal infra-red images indicate the presence of positive thermal anomalies that are associated with the large linear structures and the mechanism of Quchan-Shirvan fault system conforming to the active tectonic of this zone. Thermal anomalies of these images have a diffuse pattern around fault system and also have revealed 5 major linear and arcuate faults, of which the three are hidden and have not yet been distinguished in the field surveys. These linear anomalies are clearly conformed to the Quchan fault termination in north of Quchan city (Fig. 6).

Although, the relationship between thermal anomalies and large linear structures (as an earthquake precursor) is well documented in numerous papers, detecting hidden active faults and fault termination mechanism using satellite data is an innovative work.

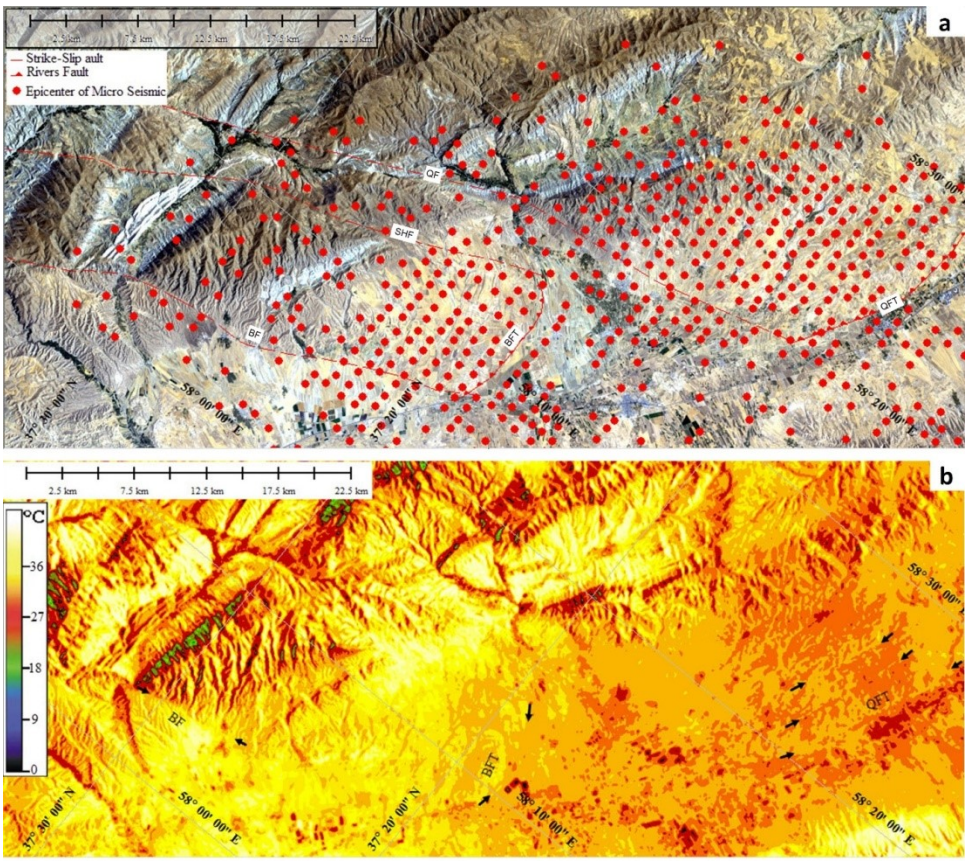

Fig. 6. (a) Landsat-8 image showing epicenters of October 2016 micro-seismic earthquakes (earthquakes with a magnitude of less than 2.0) (According to local seismic network report). BF, Baghan fault; BFT, Baghan fault termination; SF, Shokranlou Fault; QF, Quchan Fault; QFT, Quchan Fault Termination. (b) Spectral radiation of thermal image of Landsat-8 imagery (band 11), 04 October 2016 and its Emissivity imagery obtained. Arrows show the trending of hidden and active faults that they are being consistent with the Baghan (one of the Bakhardan-Quchan active fault) and Quchan fault terminations. Micro seismic scatter and Positive thermal anomaly shows that these faults are active.

6. A model for active faulting and folding

Fig (7a) shows a drainage pattern on the fold crest (Quchan anticline), which currently have large catchment. The original rivers must have drained southward on the topography slop direction, but were affected and deflected by the anticline uplift. In Quchan fault termination, all rivers are extended along the thrust faults and deflected towards the west, where they drain on the backside of the anticline (Fig. 7a). The 3 detected lineaments on the Landsat-8 thermal image (Fig. 7b) correspond with the rivers and thrust faults trends.

Existing several ramified thrust fault along the termination of strike-slip fault, can represent elongation of fault during the time (Berberian 2005). Existing these hidden faults and drainage pattern along the anticline, give a model for the mechanism of Quchan anticline formation.

In this model, over the time and with continuance strike slip activity of Quchan fault, formation of new thrusts as a result of fault elongation and operation of compression zone along the southeast trending of Quchan fault. By the continuance of thrust activity, anticline starts to grow and older thrusts are covered with the folding sedimentary rocks and the process of thrust loadering continues until now (Fig. 8). Although this older faults are hidden and have not been observed in field survey but micro seismic activity and thermal anomaly shows that these faults are active now and as a result of this activity Quchan anticline is a growing anticline (Fig. 8).

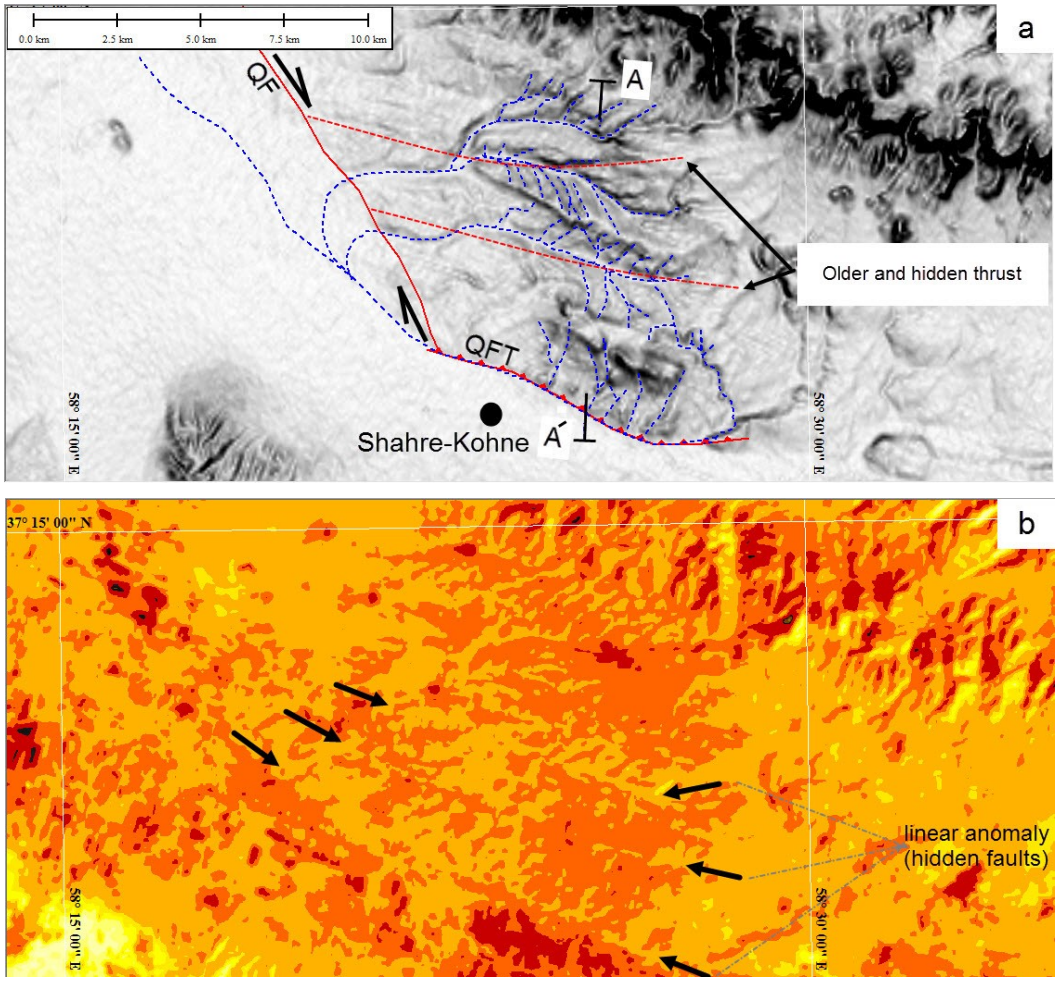

Fig. 7. (a) SRTM topography of the Quchan anticline with the drainage pattern. Rivers deflection as a result of faults activity have seen in imagery. (b) Emissivity imagery obtained from Landsat-8. Linear anomaly matches with the deflected rivers in (a) which confirmed existence of active faults along the deflected rivers.

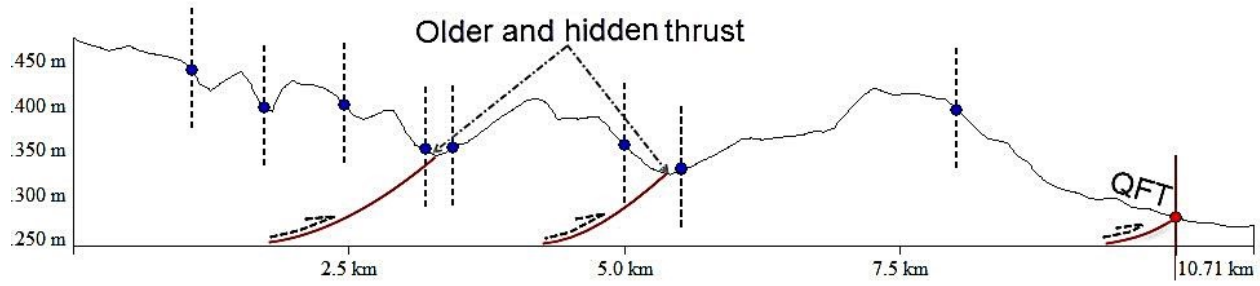

Fig. 8. The process of thrust loadering and formation of Quchan fault termination.

7. Conclusion

The neo-tectonic activities of Quchan fault in Kope-Dagh zone is testified by high-resolution Landsat-8 and TIR images, SRTM digital topographic data, field observations and micro seismicity. This activity led to the identification of a compression zone in the southeast trend of these fault followed by reverse operation of the fault terminations. The present-day right-lateral slip rates along the fault are very high and offset geomorphological landforms such as Quaternary alluvial fans, fluvial plains and drainage channels, uplift in Neocene sediment and the impact on rivers. This research is the first successful attempt in Iran to detect hidden active faults by employing satellite thermal images. In this research 3 major linear and arcuate faults are revealed using Landsat-8 thermal bands which are clearly conformed to the Quchan fault terminations. The high temperature values around these faults are synchronous with the maximum occurrences of micro-seismic earthquakes. Although, thermal anomalies near and around large linear structures are considered as earthquake precursor in numerous papers, detecting hidden active faults and fault termination mechanism using satellite data is an innovative work which has not ever been noted and worked.

Acknowledgement

We would like to thank International Institute of Earthquake Engineering and Seismology (IIEES) of Iran for access to seismic data. This research was supported by a grant from Payame Noor University (PNU), Iran.

References

Afshar Harb A (1979) The stratigraphy, tectonics and petroleum geology of the Kopet Dagh region, northern Iran. Imperial College London (University of London).

Afshar Harb A, Bolourchi M, Mehr Parto M (1987) Geological quadrangle map of Iran no. J5 (Bojnurd sheet), scale 1: 250,000, Geological Survey of Iran.

Akhoondzadeh M (2014) Thermal and TEC anomalies detection using an intelligent hybrid system around the time of the Saravan, Iran, (Mw= 7.7) earthquake of 16 April 2013, *Advances in Space Research* 53:647-655.

Allen M, Jackson J, Walker R (2004) Late Cenozoic reorganization of the Arabia-Eurasia collision and the comparison of short-term and long-term deformation rates, *Tectonics* 23.

Berberian M (2005) The 2003 Bam urban earthquake: A predictable seismotectonic pattern along the western margin of the rigid Lut block, southeast Iran, *Earthquake Spectra* 21:35-99.

Bhardwaj A, Singh S, Sam L, Bhardwaj A, Martín-Torres FJ, Singh A, Kumar R (2017) MODIS-based estimates of strong snow surface temperature anomaly related to high altitude earthquakes of 2015, *Remote Sensing of Environment* 188:1-8.

Choudhury S, Dasgupta S, Saraf AK, Panda S (2006) Remote sensing observations of pre-earthquake thermal anomalies in Iran, *International Journal of Remote Sensing* 27:4381-4396.

Cunningham WD, Mann P (2007) Tectonics of strike-slip restraining and releasing bends. In: Cunningham, W.D., Mann, P. (Eds.), Tectonics of Strike-Slip Restraining and Releasing Bends: *Geological Society Special Publication*, 290: 1–12.

Freund F, Keefner J, Mellon J, Post R, Takeuchi A, Lau B, La A, Ouzounov D Enhanced mid-infrared emission from igneous rocks under stress. In: *Geophysical Research Abstracts*, 2005. p 09568

Hollingsworth J, Jackson J, Walker R, Gheitanchi MR, Bolourchi MJ (2006) Strike-slip faulting, rotation, and along-strike elongation in the Kopeh Dagh mountains, NE Iran, *Geophysical Journal International* 166:1161-1177.

Hollingsworth J, Jackson J, Walker R, Nazari H (2008) Extrusion tectonics and subduction in the eastern South Caspian region since 10 Ma, *Geology* 36:763-766.

Huber H (1977) Geological map of Iran, scale 1: 1,000,000, National Iranian Oil Co, Tehran, Iran

Kim Y-S, Peacock DCP, Sanderson DJ (2004) Fault damage zones. *Journal of Structural Geology* 26, 503–517.

Lu X, Meng Q, Gu X, Zhang X, Xie T, Geng F (2016) Thermal infrared anomalies associated with multi-year earthquakes in the Tibet region based on China's FY-2E satellite data, *Advances in Space Research* 58:989-1001.

Lyberis N, Manby G (1999) Oblique to orthogonal convergence across the Turan block in the post-Miocene, *AAPG bulletin* 83:1135-1160.

McKenzie D (1972) Active tectonics of the Mediterranean region, *Geophysical Journal International* 30:109-185.

Pulinets S, Ouzounov D, Ciraolo L, Singh R, Cervone G, Leyva A, Dunajecka M, Karelin A, Boyarchuk K, Kotsarenko A Thermal, atmospheric and ionospheric anomalies around the time of the Colima M7. 8 earthquake of 21 January 2003. In: *Annales Geophysicae*, 2006. vol 3. pp 835-849.

Robert AM, Letouzey J, Kavoosi MA, Sherkati S, Müller C, Vergés J, Aghababaei A (2014) Structural evolution of the Kopeh Dagh fold-and-thrust belt (NE Iran) and interactions with the South Caspian Sea Basin and Amu Darya Basin, *Marine and Petroleum Geology* 57:68-87.

Sabins F (1998) Remote Sensing, Principles and Interpretation, Third edition, Freeman and company, New york, 494 pp.

Saraf A, Choudhury S (2005) Cover: Satellite detects surface thermal anomalies associated with the Algerian earthquakes of May 2003, *International Journal of Remote Sensing* 26:2705-2713.

Shabanian E, Siame L, Bellier O, Benedetti L, Abbassi MR (2009) Quaternary slip rates along the northeastern boundary of the Arabia-Eurasia collision zone (Kopeh Dagh Mountains, Northeast Iran), *Geophysical Journal International* 178:1055-1077.

Tchalenko J (1975) Seismicity and structure of the Kopet Dagh (Iran, USSR), Philosophical Transactions of the Royal Society of London A: Mathematical, *Physical and Engineering Sciences* 278:1-28.

Tronin A (1996) Satellite thermal survey—a new tool for the study of seismoactive regions, *International journal of remote sensing* 17:1439-1455.

Vernant P, Nilforoushan F, Hatzfeld D, Abbassi M, Vigny C, Masson F, Nankali H, Martinod J, Ashtiani A, Bayer R (2004) Present-day crustal deformation and plate kinematics in the Middle East constrained by GPS measurements in Iran and northern Oman, *Geophysical Journal International* 157:381-398.

Vrabel J (1996) Multispectral imagery band sharpening study, *Photogrammetric Engineering and Remote Sensing* 62:1075-1084.